Article

Improvement Strategies for Microclimate and Thermal Comfort for Urban Squares: A Case of a Cold Climate Area in China

Haiming Yu [1], Hiroatsu Fukuda [1], Mengyuan Zhou [1] and Xuan Ma [2],*

1 Faculty of Environmental and Engineering, The University of Kitakyushu, Kitakyushu 808-0135, Japan; yuhaiming515@gmail.com (H.Y.); fukuda@kitakyu-u.ac.jp (H.F.); zmyzmy11311@gmail.com (M.Z.)
2 Department of Architecture Design, Chang'an University, Xi'an 710064, China
* Correspondence: mxozil@yahoo.com

Abstract: Urban squares are an important part of a city's overall spatial environment. However, many urban squares lack rational designs, causing the thermal environment to deteriorate. To ensure sustainable urban development, urban square microclimates should be improved. Given that, this study investigates the effects of three coverages of three landscape elements of urban squares through modeling and simulation using the ENVI-met model validated by field measurements. The correlation between physiological equivalent temperature (PET) and different amounts of landscape elements is investigated using Spearman analysis. This study presents a case study of a typical urban square in a cold climate area. Design strategies in the area are proposed. The results show that the microclimate and thermal comfort of the urban square can be improved by expanding water bodies, modest increasing buildings and optimizing vegetation. Vegetation is the most important landscape element affecting thermal comfort in the urban square. The PET can be reduced by about 1.5 °C by increasing the vegetation cover from 40% to 70%. However, the degree of microclimate regulation by vegetation is disturbed by water bodies and buildings ($|\rho| \geq 0.5$). Therefore, to achieve a more comfortable thermal environment, a combination of landscape elements should be considered.

Keywords: thermal comfort; microclimate; urban square; landscape elements; ENVI-met simulation

1. Introduction

Large-scale climate projections show a strong trend of increasing temperatures over the next few decades, including all-day temperature increases, longer warm periods and more intense heatwaves [1]. As temperatures rise in the future, extreme weather events will become increasingly common [2]. Urban populations will be at greater risk from the impact of the urban heat island (UHI) effect, including low-quality outdoor environments [3], atmospheric pollution [4], risks to human health [5] and increased energy consumption in buildings [6]. At present, much progress has been made in designing strategies to reduce the impact of indoor comfort on occupants [7]. However, due to the complexity of outdoor environments compared to indoor environments, the thermal comfort of open spaces has not been adequately studied [8]. As part of cities, the mitigation of UHI effects in urban open spaces is necessary to improve the outdoor thermal comfort of residents. Outdoor thermal comfort affects a person's physical stress and emotional calmness, which are important for the user's choice of space. The most important climatic factor affecting outdoor thermal comfort is the temperature and solar radiation in the microclimate [9–13]. Therefore, improving the urban microclimate to create a healthy outdoor thermal environment is an important topic for urban planning. Some human thermal comfort indicators based on microclimate parameters have been widely used for thermal comfort assessment in different outdoor climate regions, such as Standard Effective Temperature (SET*) [14] and physiological equivalent temperature (PET) [15]. Urban squares are an important part of urban open space and the main venue for outdoor activities. In recent years, with the

development of urbanization, many large squares have been built in China and other countries, but these spaces need improvement [16]. Since people are exposed to the outdoors for long periods when using urban squares, improving the thermal comfort of urban squares has become a top priority for urban designers.

Previous research has shown that urban landscape configurations can effectively alter outdoor thermal environments at the microscale to mitigate the UHI effect [17]. It is evident from various research that vegetation and shading facilities can be used as an effective method to improve thermal comfort in urban squares. Research in Germany showed that maximizing the surface area of tree shade could provide a 5.2% cooling effect on a local urban square at 15:00 [18]. Another example of vegetation is in the United States, in California, where increasing vegetation was the most effective daytime strategy for extreme and average days. The maximum cooling temperature of vegetation reached −3.5 °C on extreme local days [19]. In Argentina, the concentration of 60 percent of the forest land around closed centers is the most effective program for the restoration of memorial squares [20]. There is also a growing amount of literature that suggests that the height of buildings plays an important role in the quality of the thermal environment. Changing building height has been reported to result in significant changes in surrounding thermal comfort [21,22]. The tallest buildings can provide more comfortable thermal conditions when they are in the center of the layout [23]. Similarly, the thermal comfort of an area can be improved by increasing building coverage [24]. However, over-increasing building coverage can lead to the deterioration of thermal comfort [22]. Finally, although few studies have discussed the design of water bodies in urban plazas, in general, water bodies are an essential element in urban areas. A study in Iran showed that evaporative cooling of water is an effective strategy to improve microclimatic conditions in urban squares in temperate and arid regions [25]. From a case in Italy, it was seen that expanding water surfaces could reduce the temperature of a city square in the center of Rome by 0.9 °C. Locally, the expansion of water surfaces improved thermal comfort, which was second only to the improvement of vegetation [12].

In general, previous studies have provided a lot of new insight into the variation of thermal comfort in urban squares, such as exploring the influence of the combination type of trees on microclimate [26–28], exploring the influence of the shape and size of water bodies on urban climate [29], the influence of building orientation on the thermal comfort of urban open spaces [30], etc. However, these studies have mainly focused on the improvements brought by optimal planning layouts, and there is a lack of quantitative studies on landscape elements. Moreover, papers on this topic have generally focused on a single landscape element and still lack a systematic understanding of how multiple factors contribute to thermal comfort. This paper uses multi-factor case studies (including buildings, water bodies and vegetation) and quantitative research methods to make a comparative study of various scenarios, thus filling the gap in comprehensive research in this field. The simulation software ENVI-met was also used. Experimental data such as air temperature and relative humidity were collected by actual measurements. Boundary conditions were determined, and numerical models were calibrated.

Numerous studies have confirmed that the same measure has different effects in different zones [31,32]. Therefore, it is necessary to consider the local climate, the actual situation and the user's perception in practice. Studies on the outdoor thermal environment of squares in China have been conducted in severely cold climate areas [33], hot summer and cold winter climate areas [30] and hot summer and warm winter climate areas [34]. However, few studies have been conducted in cold climate areas due to the lack of educational resources in northern China [35]. Therefore, it is necessary to supplement the thermal comfort studies of urban squares in this area.

This study is based on climatic conditions in cold climates and has three main research objectives. The first objective is to assess and rank the impact of three configurations of three landscape elements on microclimate parameters in urban squares; the second objective is to assess the correlation between the impact of building coverage, water coverage and

vegetation coverage on thermal comfort and to explore its internal mechanisms; and the third objective is to develop and test the applicability of various thermal environment improvement design strategies to provide a reference for urban designers.

2. Materials and Methods

2.1. Research Area

Xi'an is located between 107°40′–109°49′ E and 33°39′–34°45′ N. It is geographically located in the center of China. Among the five climate areas in China, Xi'an is a typical city in a cold climate area. A cold climate area is defined as an area with an average temperature of the coldest month being −10–0 °C and the average daily temperature being ≤5 °C for 90–145 days [36]. For a long time, urban planning and construction in cold climate areas have focused on keeping warm in winter, and little attention has been paid to the heat in summer. The historical meteorological data of Xi'an are shown in Table 1. Xi'an has a hot summer with a significant UHI effect, which is not conducive to the daily life and outdoor activities of residents.

Table 1. Historical weather in Xi'an (from May 2020 to May 2021).

Item	AT (°C)	RH (%)	WS (m/s)	Hours of Daylight (h)
Avg	15.5	61	2.1	12
Min	−10.0	19	0.1	9
Max	38.5	88	9	14

The Big Wild Goose Pagoda Square was built in 589 A.D. After more than 1000 years of rising and falling and expansion, it is an iconic square in Xi'an and was listed among the World Heritage Sites in 2013 [37]. This study was conducted in the Big Wild Goose Pagoda's North Square (Figure 1). The Square is made up of a water fountain, a cultural square, a garden landscape, a cultural promenade and tourism commercial facilities, with the tower serving as the center axis. It measures 480 m east to west and 350 m north to south and covers 168,000 m^2.
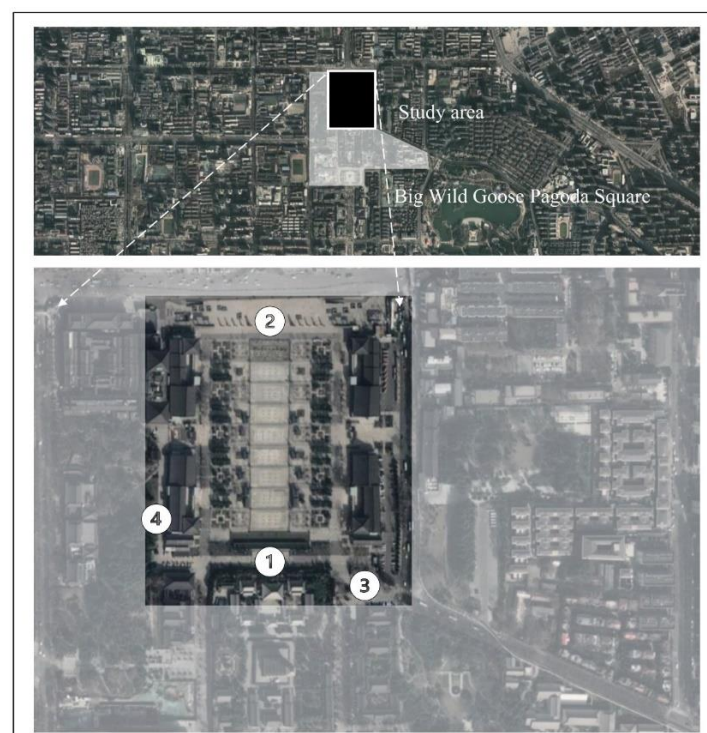

Figure 1. Study area location and Sites 1–4.

Xi'an has four distinct seasons, with the hottest month of July and the coldest month of January throughout the year. In this study, field measurements were performed in the Big Wild Goose Pagoda's North Square from 27–29 July 2020. Four measurement sites were set up at the north–south road, entrance square, east–west road and green space for this study to investigate the various influencing elements (Figure 1). Site 2 was used as a reference site because it is the closest to the boundary without the influence of shade all day. All instruments were ISO 7726 compliant and were mounted on tripods in the square at a height of 1.4 m above ground. Detailed information on the instruments is in Table 2. In addition to the measured climatic parameters, data from local weather stations were consulted. These observations were utilized to determine the microclimate conditions in the study area and served as the foundation for the square simulation model. Figure 2 shows the framework for this study.

Table 2. The specifications of the instruments that were used.

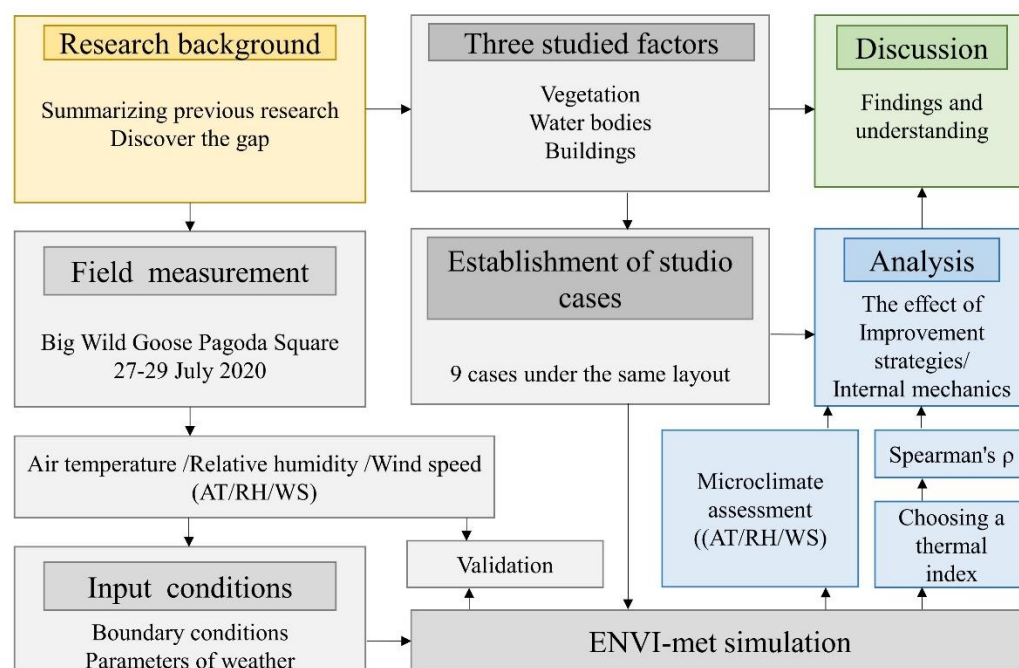| Variable	Sensor	Accuracy	Range	Interval	Mode
Anemoscope	DS-2	± 0.3 m/s	0–70 m/s	1 min	Automatic
Air temperature	TR-72wf	± 0.5 °C	$0-\pm 55$ °C	1 min	Automatic
Relative humidity	TR-72wf	$\pm 5\%$	10–95%	1 min	Automatic

Figure 2. The framework of this study.

2.2. Model Setup

ENVI-met V4.4 (ENVI-met) was used for simulations in this study. A complete ENVI-met simulation model has four subsystems (atmosphere, soil, vegetation and buildings), and the model database provides a large number of environmental parameter options [38]. The software includes a tool called "Biomet" which allows the math of various thermal comfort indexes. The ENVI-met model is one of the most widely used dynamic simulation tools for microclimate analysis. Researchers use it not only to investigate current microclimate conditions but also to compare and evaluate the effects of various strategies on UHI effects [39].

The ENVI-met model of the study area was constructed based on field surveys and aerial photographs. The horizontal modeling grid cells were 4 × 4 m, and the height was 2 m. This model was used to create a simulation model with 83 × 99 horizontal cells and

30 vertical cells. To avoid boundary effects, 5 layered grids were placed on either side of the simulation model. The materials of each element in the square were chosen based on their current state. It should be noticed that the water body in the study area includes timed fountains, which, in this study, were simplified to shallow pools because the fountains only run for 20 min during the measuring period. An actual measured uniform water depth of 0.5 m in the ENVI-met model was used because water levels greater than 0.45 m did not affect the simulation results [40].

Previous studies have emphasized that changing boundary settings, material properties and experimental protocols can improve the correlation between simulations and measurements [41,42]. In this study, the weather station was located on the outskirts of Xi'an city, far from the measurement site in the city center. To reduce the error between the simulation and measurements, the input meteorological parameters of the model needed to be modified, and the modified data were used as the original boundary condition of modeling. Upon completion of the data collection, we compared the measurements from the reference station with the data from the weather station. As shown in Figure 3a,b, the measured temperature per hour at the weather station was 1–4.5 °C below the measured data, and the RH was 3–30% percent higher than the measured data. Therefore, in this study, modified weather station data that increased the AT of the weather station by 7% and decreased the RH by 20% were used as the input data for the model. Table 3 shows the microclimate simulation settings and meteorological parameters that were entered by the model in ENVI-met.
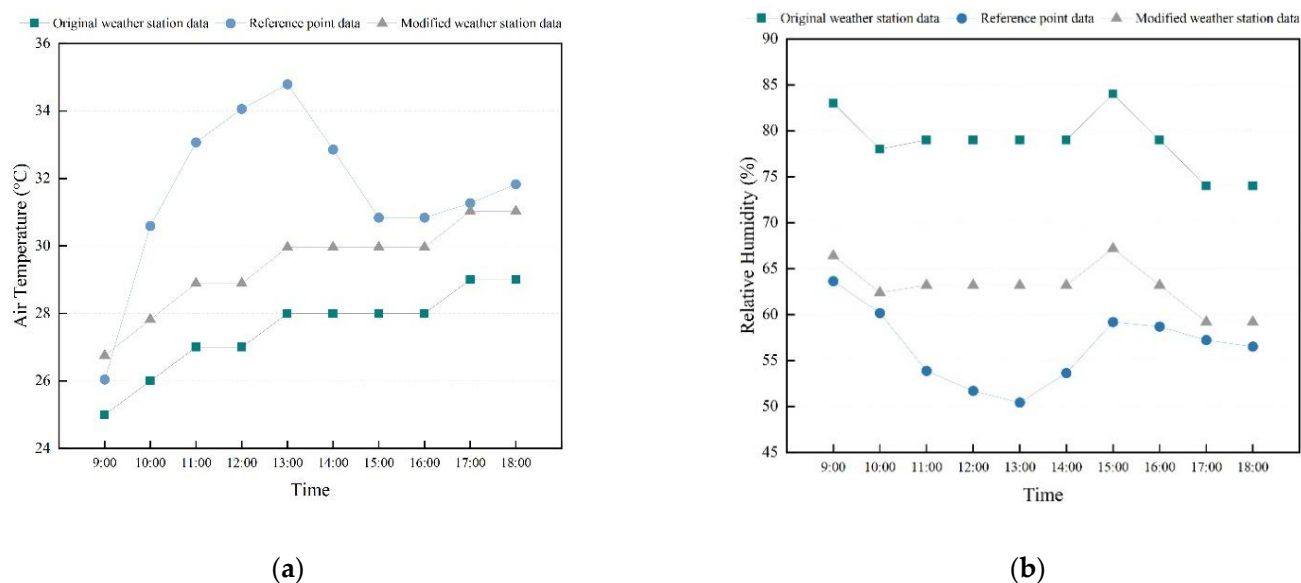

(**a**)

(**b**)

Figure 3. The comparison of the reference point data and weather station data: (**a**) AT; (**b**) Rh.

Table 3. Microclimate simulation settings and meteorological parameters of the model input in ENVI-met.

Parameters	Values Used
Simulation Date	28 July 2020
Simulation Time	2:00 a.m.–6:00 p.m.
Total Simulation Time	18 h
Simulation Level	Intermediate
Boundary Condition	Simple Forcing
Wind Speed at 10 m	4 m/s
Wind Direction	45 Northeaster
Roughness Length	0.01
Initial Air Temperature Range	Modified weather station data
Initial Relative Humidity Range	Modified weather station data

2.3. Redesign Model

The current coverage of water bodies, vegetation and buildings in the study area is 10%, 20% and 15%, respectively. Previous studies have concluded that people prefer to be exposed to green spaces with water [43]. According to the characteristics of the cultural theme square, more than 80% of these spaces are designed with water bodies. The average proportion of water area ranges from 5% to 25%, with a minimum of about 5% and a maximum of about 30% [44]. On this basis, the water coverage in the model was redesigned to 5% and 30% to compare with the current coverage of the study area (10%). These cases are symbolized by W5%, W10% and W30%, as shown in Figure 4a. Greenspace has been identified as an important factor influencing the landscape preference of the square [45]. According to the Chinese urban green space classification standard, the percentage of the green area is classified as less than 35%, 35% to 65% and greater than 65% [46]. Based on this criterion, the model was redesigned to 40% and 70% for comparison with the status quo (20%). These cases are symbolized by T20%, T40% and T70%, as shown in Figure 4b. Previous studies have proven that building thermal comfort for the whole day outdoors is mainly affected by building height, and building distance and layout form have negligible effects on the average outdoor thermal comfort of spaces [47,48]. Buildings in the study area are currently predominantly two-story, with some single-story structures and a building coverage of 15%. Considering the influence of building coverage and height on the thermal environment of the site, the building coverage was redesigned to 5% and 30% to compare with the current situation (15%). These cases are symbolized by B5%, B15% and B30%, as illustrated in Figure 4c.
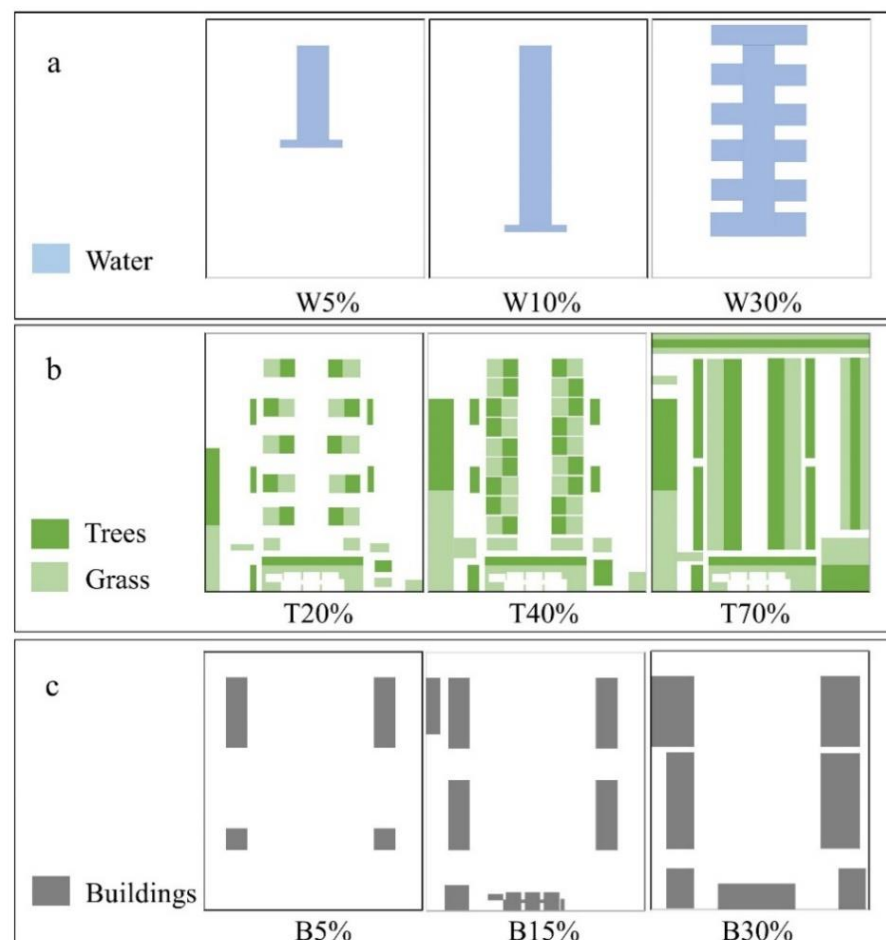

Figure 4. Redesigned scenarios of the (**a**) water bodies, (**b**) trees and (**c**) buildings of the square.

2.4. Thermal Comfort Index

In the 55th ASHRAE Standard, human thermal comfort is clearly defined as a psychological state of satisfaction with the thermal environment [49]. The relationship between physiological factors and outdoor thermal comfort begins with heat exchange between the body and its surroundings. In normal times, people can dissipate heat by evaporation, convection and heat transfer to maintain heat balance with their surroundings [50]. This thermoregulatory activity can change the physiological parameters of the body accordingly. Therefore, given the correlation between physiological parameters and thermal comfort, although human thermal comfort is a subjective feeling, the relevant physiological parameters can be used as an objective evaluation indicator of human thermal comfort [51]. Dozens of thermal comfort evaluation criteria can be used for reference by researchers, including many thermal comfort evaluation criteria based on the steady-state heat transfer model and dynamic heat transfer model [52,53]. Over the last two decades, thermal comfort research has moved toward more complex dynamic conditions [54]. Thermal comfort prediction methods can be divided into three categories: (1) thermal equilibrium methods (mainly laboratory studies); (2) adaptive regression models (mainly field studies); and (3) adaptive heat balance [52].

Several common metrics such as Standard Effective Temperature (SET*) [14], Predicted Average Vote (PMV), General Thermal Climate Index (UTCI) [55] and Physiological Equivalent Temperature (PET) [15] have been developed to evaluate thermal comfort in different types of outdoor environments [56,57]. Based on the existing literature review, PET and UTCI are the main evaluation indices that can fit cold climate areas [58]. Physiologically equivalent temperature (PET) has been used more frequently in outdoor thermal comfort studies in recent years because it is the only one that can be applied to a variety of climate areas with temperatures ranging from -50 to 50 °C [15]. Many studies have demonstrated that the range of thermal comfort varies with area [40,59–61]. Since both Tianjin and Xi'an belong to a cold climate area, the PET adapted to the local climate of Tianjin, as modified by D Lai et al., which was used as a criterion for evaluating the thermal environment in this study (Table 4) [62].

Table 4. Relationship between thermal sensation and PET for Tianjin residents in cold climate areas.

| Thermal Sensation	PET Range (°C)
Very cold	<-16
Cold	-16 to -11
Cool	-11 to -6
Slightly cool	-6 to 11
Neutral	11 to 24
Slightly warm	24 to 31
Warm	31 to 36
Hot	36 to 46
Very hot	>46

3. Results and Analysis

3.1. Simulation Data Validation

In this study, a statistical analysis of the simulation and measurement data was performed using the Statistical Package for the Social Sciences (SPSS). As previous studies have proposed, AT and relative humidity RH have been used to test ENVI-met models as important microclimate parameters [12,63]. Therefore, the ENVI-met model was validated using AT and RH measurements from the four sites. The results are considered more accurate when the root-mean-square deviation (RMSE) values approach zero and when R^2 values approach one. Figure 5 shows a comparison between the simulated model and the field data. It was calculated that the RMSE in AT was 0.92 °C and that the RMSE in RH was 1.061. In the ENVI-met model of simple force, the measurement deviated from the simulation, which may be attributed to the static cloud and wind condition assumptions. In

addition, inadequate measurements of air flow [64], wall and roof material properties and the use of default modeling were also contributing factors. Nevertheless, the RSME values that were obtained in the current study are in the range of those summarized by Salata et al. in a recent review of ENVI-met simulations (RMSE in AT is less than 4.30 °C, and RMSE in RH is less than 10.2) [65]. In addition, as shown in Figure 5a,b, the R^2 in AT and RH were 0.79 and 0.86, indicating a high correlation between the measured and simulated values. The above data analysis shows that ENVI-met can be applied to the microclimate simulation of Xi'an urban squares.
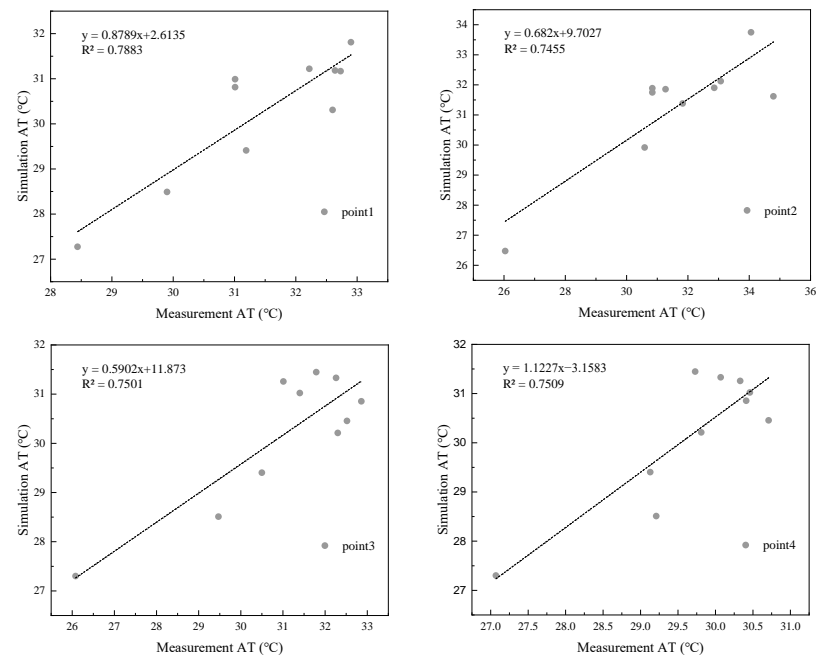
(**a**)
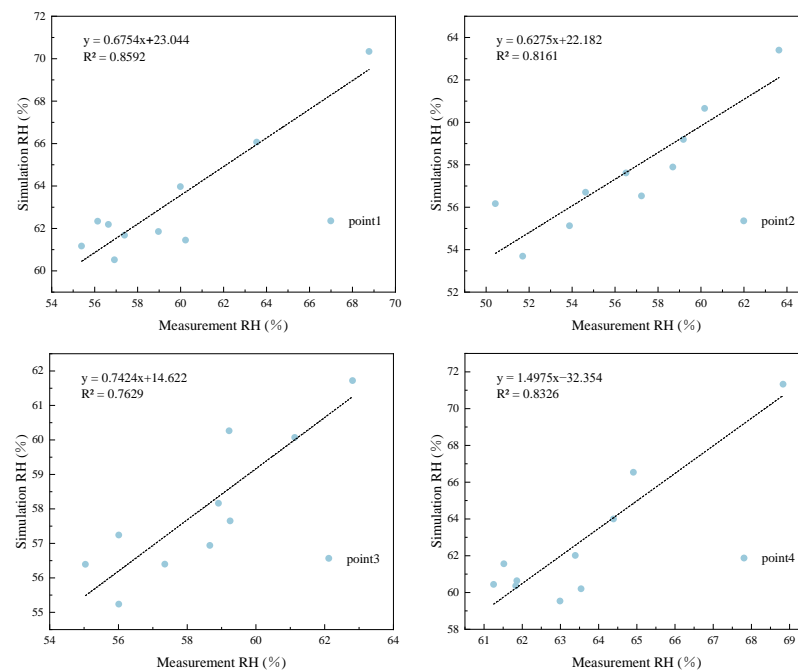
(**b**)

Figure 5. Linearity between the simulated data and the measured data: (**a**) AT; (**b**) RH.

3.2. PET Distribution in the Status Quo

The PET values were calculated for the research area by Biomet. As previous studies have proposed, the worst thermal comfort conditions always occur between 14:00 and 16:00 [30,66,67], both in real measurements and in ENVI-met modeling. Figure 6 shows the PET values for the north square of the Big Wild Goose Pagoda from 9:00 to 18:00. Since the distribution of PETs within each hour does not satisfy a normal distribution, the mean of this data set is more representative than the median. The line of the means shows that the mean PET values in the study area were the highest at 14:00, reaching "very hot" (PET > 46 °C) in summer. Therefore, this section focuses on the microclimate and thermal comfort of the square at 12:00.
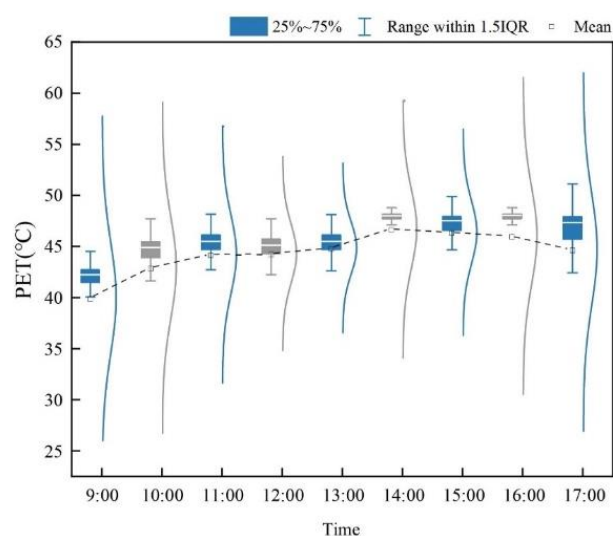

Figure 6. PET variations at different times.

3.3. Microclimate Conditions of Redesigned Cases

The ENVI-met model was tested in Section 3.1, and it was shown to provide convincing simulation results. Given this, simulations can be used as an alternative to realistic reconstructions. ENVI-met was used to simulate and test the effects of microclimate and thermal comfort modifications in the redesigned study area. According to the redesigned scheme (Figure 4), the correlated ENVI-met model was built and simulated to obtain the spatial and temporal distributions of microclimate data, including AT, RH and WS. The PET values were calculated for the four measurement sites by Biomet.

3.3.1. The Impact of Differing Water Coverage on the Microclimate Parameters

The distribution maps (Figure 7) of microclimate parameters (AT, RH and WS) show that increasing the coverage of the water body effectively changes the AT above and near the water, and the temperature distribution within the square decreases with distance from the water body for all three cases. This is because the specific heat capacity of water is greater than that of the ground. Comparing the three cases, we can see that adding water bodies at different locations in the square also has different effects, with the downwind areas of the square being more influenced by the water bodies than the upwind areas. It is also clear that there are spatial differences in the effects of increasing the water area on AT. For example, the cooling effect was greater in the not-under-tree space than in the under-tree space. The difference in RH due to increasing water coverage was more obvious than the difference in AT. The difference in RH between the water body and the ground stems from their difference in evaporation capacity.
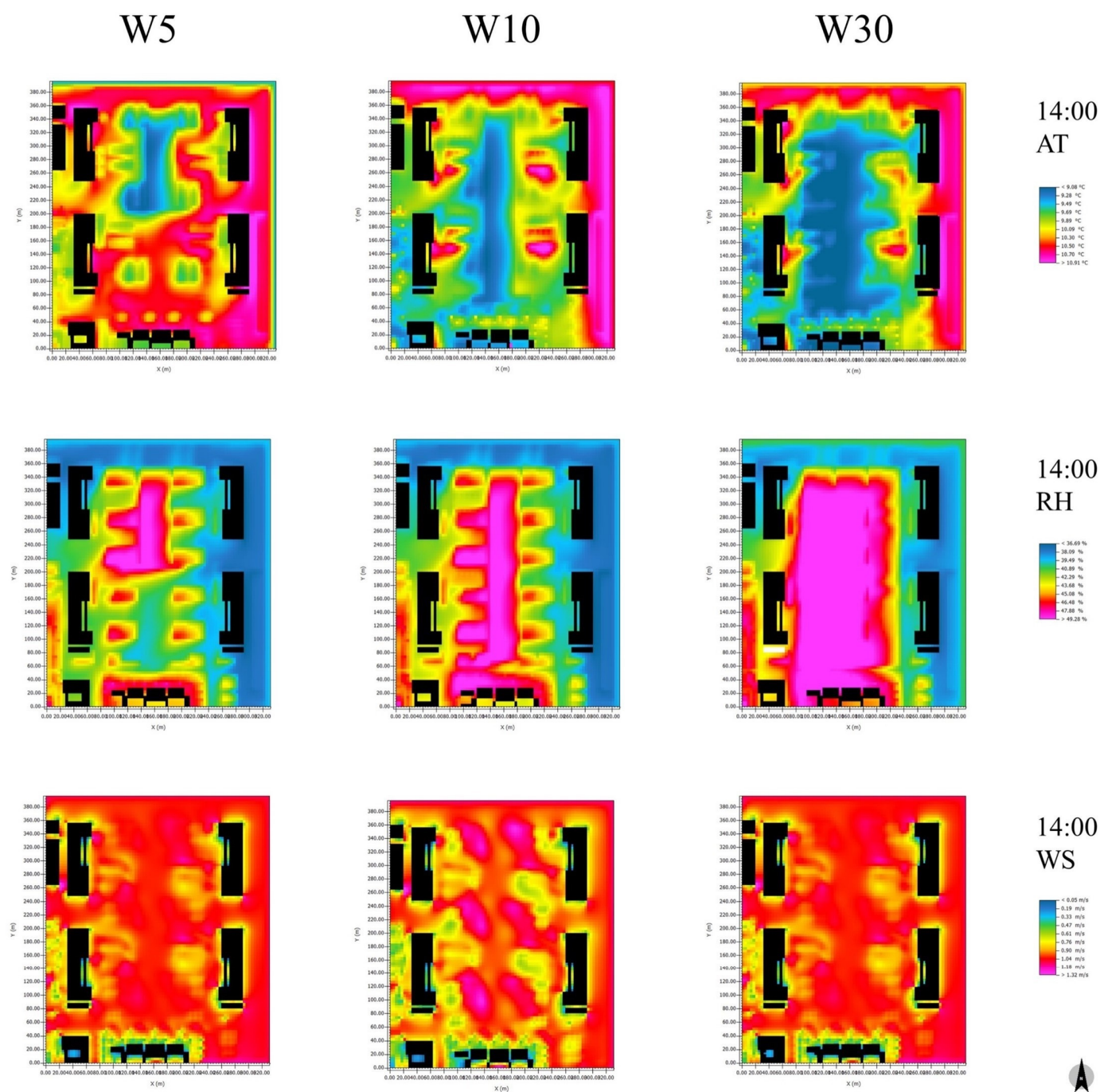
Figure 7. Distribution maps of microclimate parameters at 14:00 with redesigned water body coverage.

With respect to wind speed, as shown in Figure 7, the difference in wind speed between the three cases was less than 0.06 m/s. The increase in water area changed the surface roughness, resulting in a slight change in wind speed. The difference in temperature between land and water resulted in different wind speed trends. In general, an increase in water body coverage led to a decrease in AT, an increase in RH and a slight change in WS. Therefore, an appropriate increase in water area can provide an effective cooling effect in the design of urban squares.

3.3.2. The Impact of Differing Vegetation Coverage on the Microclimate Parameters

Previous studies have demonstrated that the increased canopy density of vegetation attenuates the effect of solar radiation and decreases AT [68]. In this study, the distribution

of microclimate was investigated for vegetation coverage of 10%, 40% and 70%. The results show that the relationship between vegetation coverage and AT in the square followed this pattern (Figure 8). Moreover, the effect of vegetation coverage on AT had spatial differences. For instance, because buildings block part of the solar radiation, the cooling effect of vegetation is reduced under building shade [69,70]. In addition, vegetation has different cooling effects around buildings with different orientations. As shown in Figure 8, the cooling effect of vegetation around the east–west oriented buildings was better than that of the north–south oriented buildings. With respect to relative humidity, vegetation converts liquid water into water vapor by transpiration to reduce the temperature and thermal comfort of leaves and surrounding air. The effect of RH by changes in vegetation coverage was pronounced in the summer.
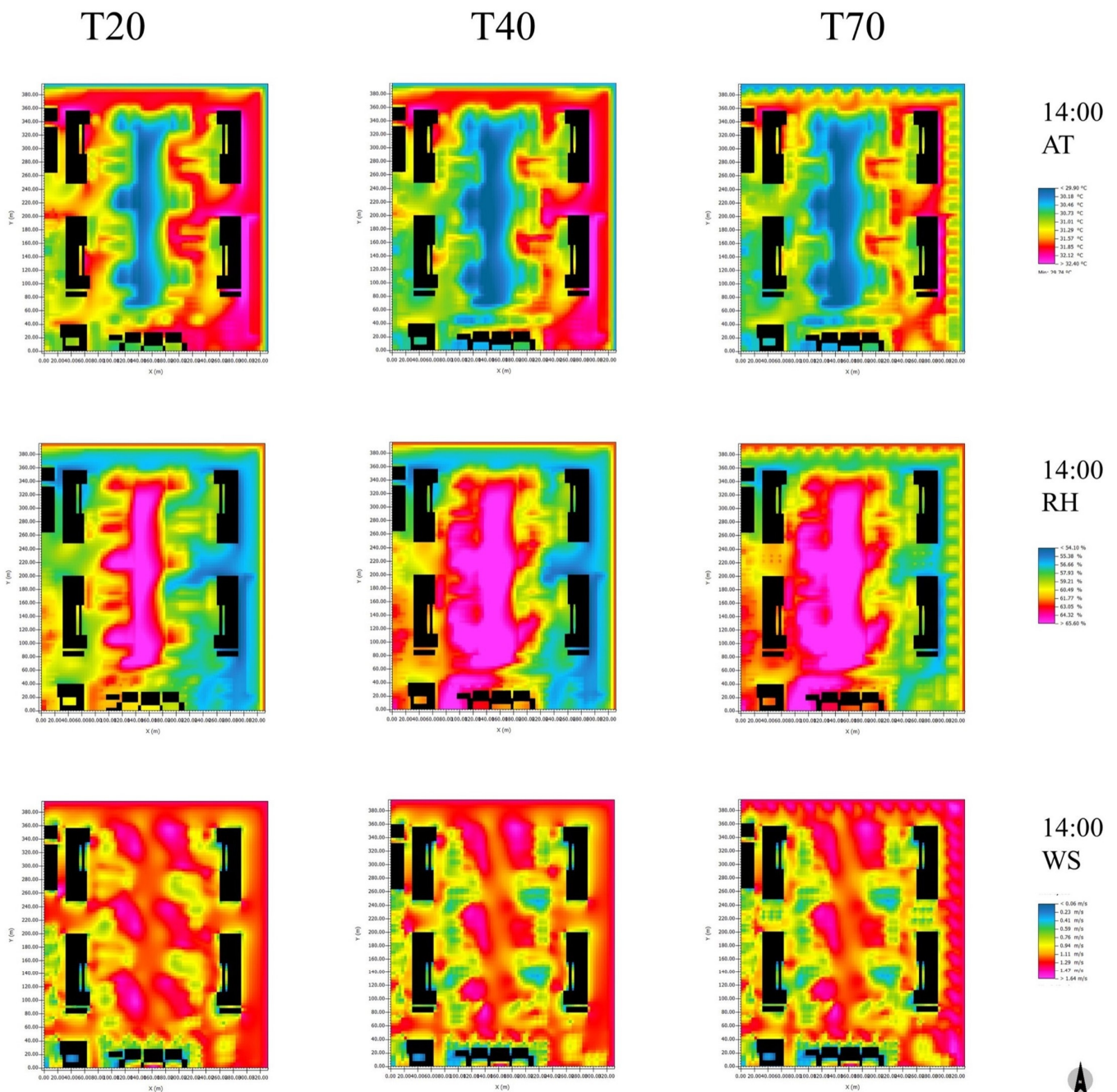

Figure 8. Distribution maps of microclimate parameters at 14:00 with redesigned vegetation coverage.

With respect to wind speed, the temperature difference caused airflow, resulting in a weak change in wind speed in the area where trees increased or decreased. WS was reduced in increased arborization because the dense tree canopy blocked the wind flow. Since this variation difference is less than 0.15 m/s, it can be considered negligible. In general, because the wind environment is quiet all year in cold climate areas, changing the vegetation coverage of the square has no significant effect on the WS in summer.

3.3.3. The Impact of Differing Building Heights and Densities on the Microclimate Parameters

Xi'an has a long history as the capital of thirteen ancient dynasties. The planning of the modern city of Xi'an still retains the style of the ancient capital city, following the layout of horizontal and vertical streets and symmetrical buildings. The vertical layout of the building complex is mostly north–south oriented, with the main building in the middle. The ancillary buildings are oriented east–west and are located on either side. The overall height of the complex is high in the north and low in the south. The layout of the study area also follows this style. It has been demonstrated that different urban spatial patterns lead to multiple reflections of solar radiation between buildings, which affects the flow of wind in the city and ultimately the dissipation of heat within the city [42]. In case B30%, the accumulated solar radiation was absorbed, and the heat that was released into the surrounding space was greater than it was in the other two cases as the buildings increased overall, resulting in a higher AT in this case than in the other two cases. For the overall square, the buildings caused changes in the thermal environment mainly by affecting solar radiation. In this study, although buildings have a local impact on the thermal environment through their processes of absorbing, releasing and blocking heat, the AT of the whole square was not significantly affected by changing the building height and density (Figure 9).

With respect to relative humidity, a comparison of the three cases reveals that the changes in building height and density caused only slight changes in the RH distribution within the square. With respect to wind speed, past studies have shown that increasing building height and density decreases the overall wind speed. In this study, B30% was the case with the largest building coverage and height. In the summer, the wind speed distribution of B30% was lower than it was in the other two cases. The increase in buildings increased the wind shadow area in the vicinity, which led to a decrease in WS in the wind shadow area.

3.4. Thermal Comfort of Redesigned Cases

Since sites 2 and 4 are more representative, the PET values were calculated and compared between 9:00 and 18:00 for sites 2 and 4 after the square redesign (Figure 10). Figure 6 shows that the thermal comfort of the study area in summer is classified as "very hot" after 12:00. The PET values in the redesigned square did not decrease significantly, but the human comfort was reduced from "very hot" to "hot". This indicates that the redesign of the square had a moderating effect on thermal comfort. For instance, as shown in Figure 10, rising vegetation coverage usually improves thermal comfort in summer.
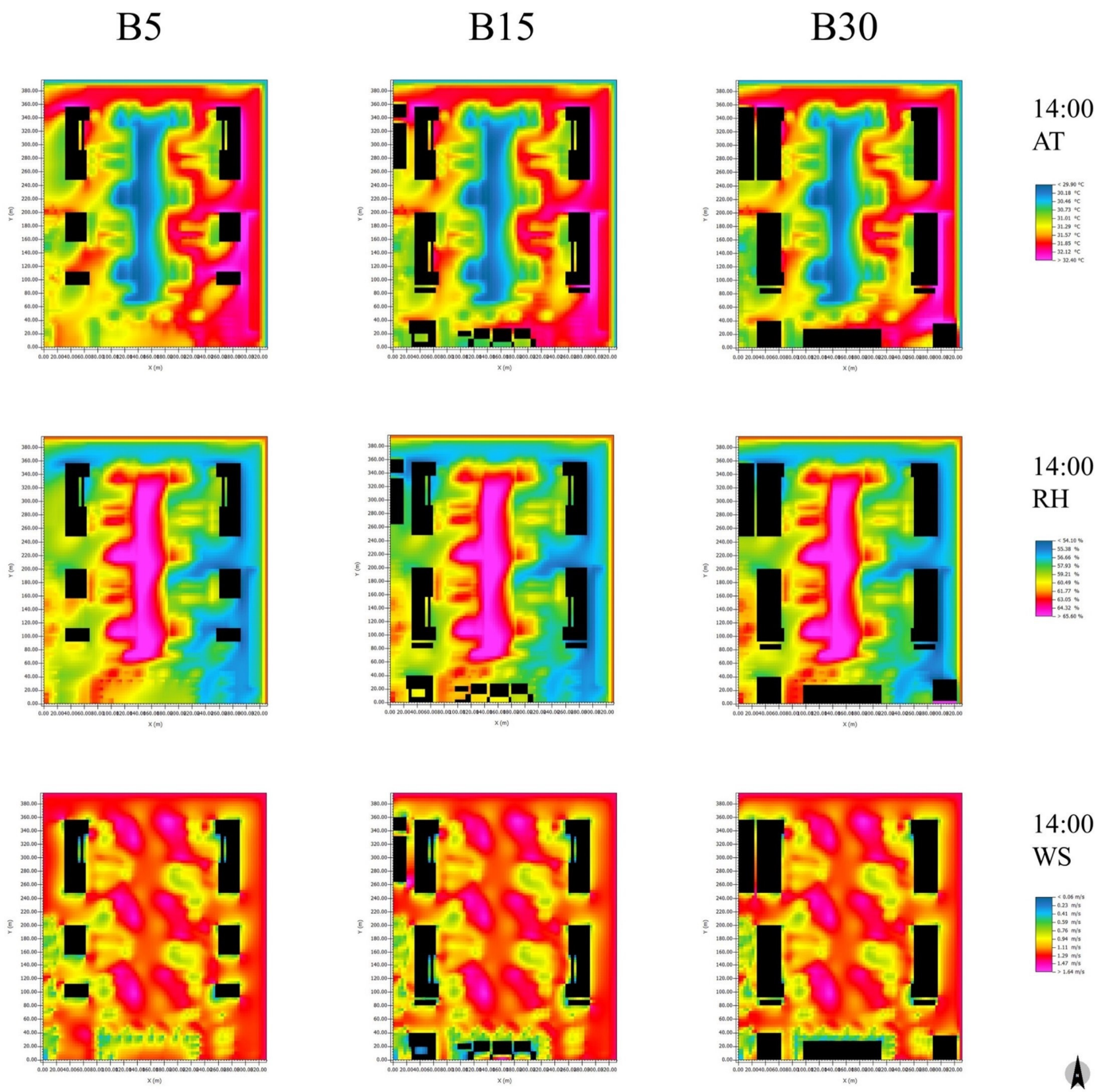
Figure 9. Distribution maps of microclimate parameters at 14:00 with redesigned building heights and densities.
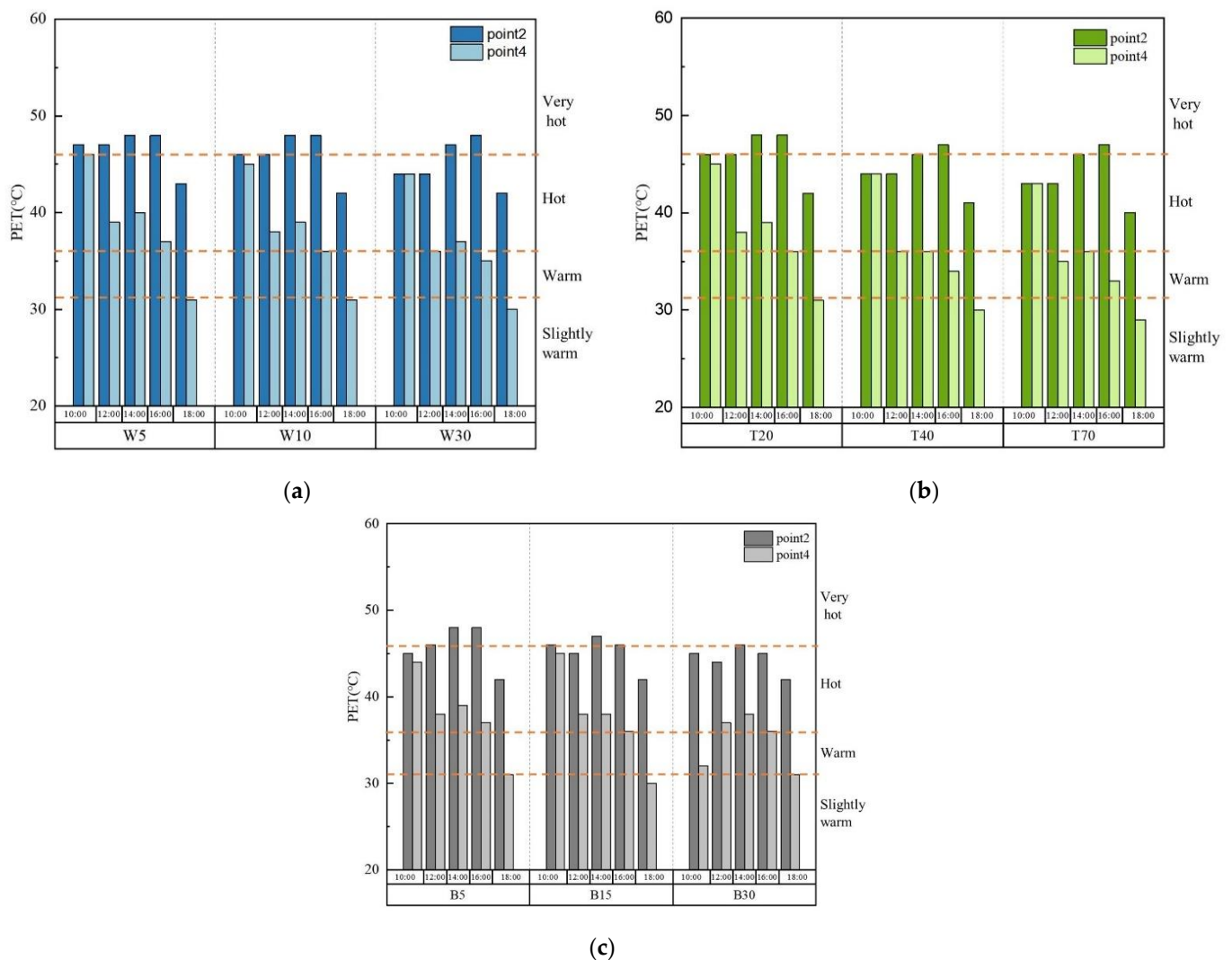
Figure 10. Time course of PET values at sites 2 and 4 in the redesigned cases: (**a**) water bodies; (**b**) vegetation; and (**c**) buildings.

3.5. Internal Mechanics

The simulation results show that the thermal comfort regulation effect of a single landscape element can be influenced by other landscape elements (Figures 7–9), For example, the cooling effect of trees was lower near buildings than it was in open spaces. Therefore, increasing the understanding of the correlation between landscape elements can help to improve their thermal comfort enhancement efficiency. A correlation analysis is an analysis of the degree of correlation between two variables. There are three ways to calculate the correlation analysis, which are Pearson's correlation coefficient, Spearman's correlation coefficient and Kendall's tau-b correlation coefficient. In this study, the correlation between the effects of vegetation, water bodies and buildings on PET was analyzed. It was necessary to test whether each variable conformed to a normal distribution to select a suitable analysis method. Since the median deviation from the mean was large and most of the variables did not conform to a normal distribution, Spearman correlation analysis (Spearman's ρ) was used. In statistics, Spearman's rank correlation coefficient is named for Charles Spearman. The rank score can be introduced in a correlation analysis when the data do not satisfy the normal distribution, or when some quantities cannot be expressed in the data [71]. More specifically, the two variables are first sorted to obtain the corresponding rank numbers, and the rank numbers are used to replace the original data and are then brought into the Pearson correlation coefficient formula to obtain the Spearman correlation coefficient:

$$\rho = \frac{\sum_i (X_i - \overline{X})(Y_i - \overline{Y})}{\sqrt{\sum_i (X_i - \overline{X})^2 \sum_i (Y_i - \overline{Y})^2}} \tag{1}$$

Data were assigned a corresponding rank based on their average descending position in the overall data. The PET values of site 2 from 10:00 to 18:00 in the summer are taken as an example (Table 5):

Table 5. Example for Spearman's ρ.

Variable X_i	Rank x_i	d_i
45.55	4	4
45.92	3	3
48	2	2
48.22	1	1
42.4	5	5

By subtracting the corresponding elements of the two observed variables to obtain a difference, the above equation can also be transformed into:

$$\rho = 1 - \frac{6 \sum d_i^2}{n(n^2 - 1)} \tag{2}$$

where $d_i = R(X_i) - R(Y_i)$ is the difference between the two ranks of each observation, and n is the number of observations.

Spearman's ρ is a parentless measure of two-variable dependence that uses a monotonic equation to evaluate the correlation between them. If the data do not contain any repeated values and the two variables are exactly monotonically connected, the Spearman's ρ is either +1 or −1. Spearman's ρ uses the rank order magnitude of the two variables for analysis and is a nonparametric statistical method [72]. It applies to continuous variables that do not meet the requirements of a normal distribution of Pearson correlation coefficients. It can also be used to measure the correlation between ordered categorical variables.

In this study, nine sets of cases were analyzed to clarify the internal mechanics between the three elements. The results are shown in Figure 11. There was a correlation between PET values between changes in the quantity of water bodies and buildings. The PET values were between the quantity of vegetation and water bodies, and quantity of vegetation and buildings were positively correlated. The PET values between the quantity of vegetation and water bodies had a lesser correlation, and all other elements' relationships were positive. Landscape architects are often confused by different possible choices in the design process. This finding can provide a reference for which landscape factor should be adjusted as a priority in the process of optimizing thermal comfort in completed projects. We hope that our study can provide design guidance for urban plaza landscape configurations under similar climatic conditions.
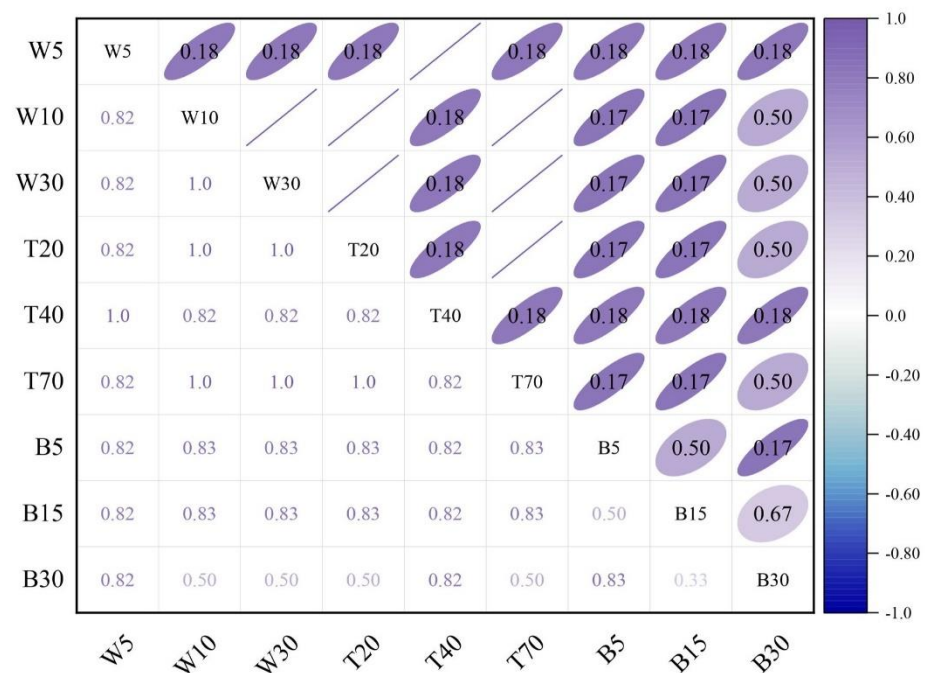
Figure 11. The Spearman's rank correlation coefficient of landscape elements based on PET.

4. Discussion

A theoretical implication that can be drawn from the third section is that the design of squares in cold climate areas should consider the coverage of landscape elements such as water bodies, vegetation and buildings. For water bodies, the rise in evaporation and ventilation due to the increase in water bodies can improve thermal comfort. It is possible to reduce the thermal comfort of a square from near "very hot" to "hot" or "warm". For vegetation, increasing the vegetation coverage usually increases the thermal comfort of the square. Therefore, the vegetation proportion design needs to be optimized to achieve the desired thermal perception. For buildings, the shading provided by buildings increases thermal comfort to some extent in the summer. For example, as shown in Figure 12, the PET value of case B30% is about 0.82 °C lower than that of cases B5% and B15%. The importance of landscape elements impacting summer thermal comfort is ranked as follows: vegetation, water bodies and buildings.

This study also explores the role of interactions among the three landscape elements. Specifically, there is a correlation between the effects of water bodies, vegetation and buildings on PET, and thus, a linear model should not be used when building the mathematical model. Water bodies and buildings do not influence each other to a high degree on the site's PET, so designers do not have to consider the effect of the combination of these two elements when designing. In contrast, the influence brought by vegetation can be influenced by both water bodies and buildings, which prompts designers to give special consideration to the location of vegetation when designing a square. In the summer, there is a slight interaction between vegetation and water bodies, which is influenced by buildings at a higher level. At the same time, there is also an interaction between water bodies and buildings, which suggests that designers can achieve better results when choosing the right combination according to the interactions of several factors in the design.
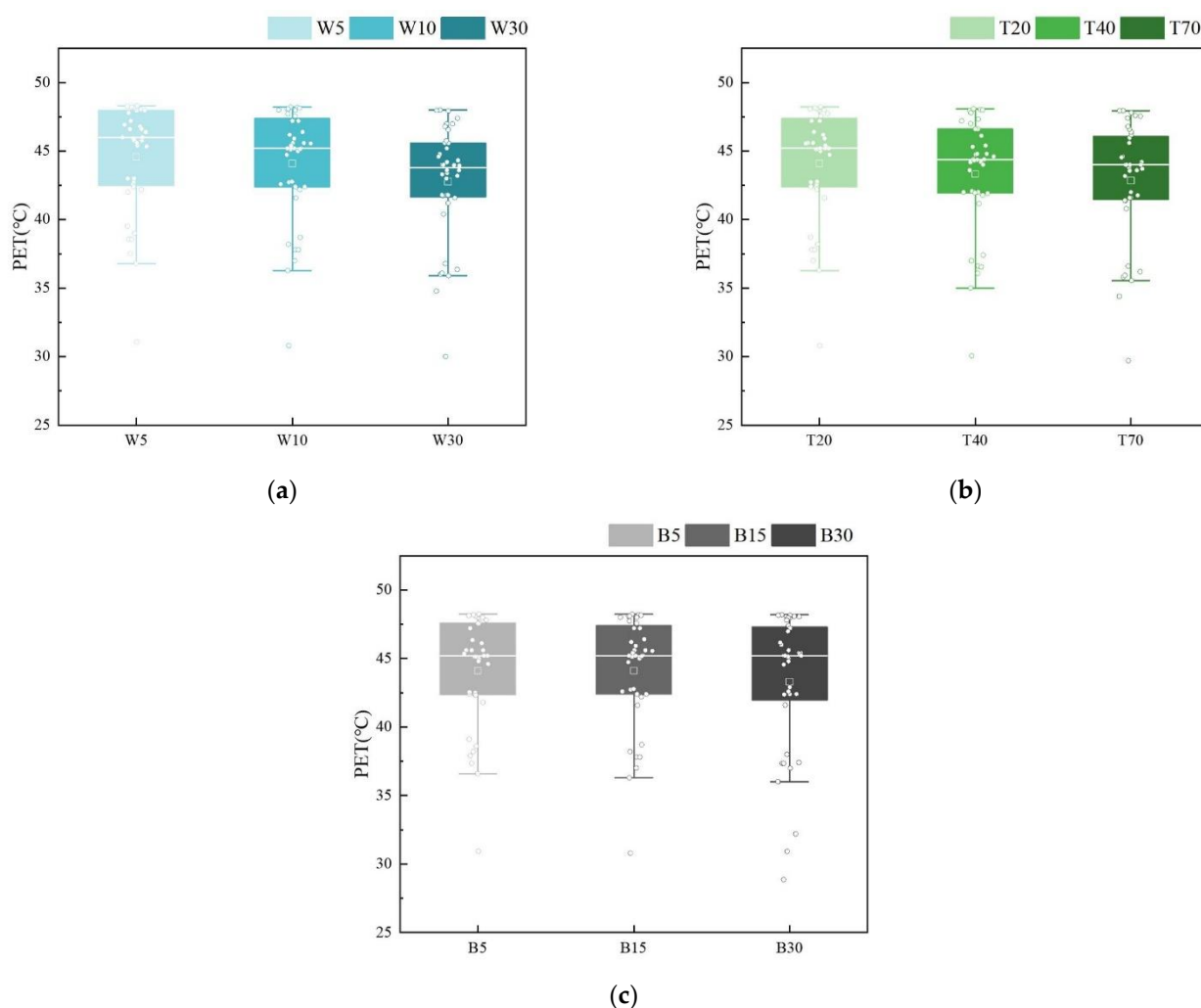
Figure 12. Box plots of PET from 9:00 to 18:00 vs. different quantities of (**a**) water bodies; (**b**) vegetation; and (**c**) buildings.

5. Conclusions

This study is a pioneering study that has successfully quantified the impact of multifactor landscape elements (vegetation, buildings and water bodies) on thermal comfort in summer urban squares. Our results successfully quantify and compare the effect of landscape element change ratios on thermal comfort improvement in urban squares in cold climate areas. The main findings of the study are as follows:

(1) Modified boundary conditions allow ENVI-met simulations to achieve convincing simulation accuracy in urban squares in cold climate areas ($R^2 > 0.78$, RMSE < 2).

(2) Increasing vegetation coverage is the most effective strategy to improve microclimate and thermal comfort, followed by increasing water coverage and modest increasing building height and density. The ranking of important landscape elements that affect thermal comfort in summer is vegetation, water bodies and buildings.

(3) There is a correlation between different types of landscape elements for thermal comfort enhancement ($|\rho| \geq 0.5$), so they should be considered together. This method of arrangement can be used by designers in the pre-planning and project renovation stages.

It should be mentioned that this study focuses on only three main landscape elements, whereas in reality, the types of elements and their interactions with microclimate conditions are much more complex, including elements such as the airflow around the perimeter of the building enclosing the square. Despite these limitations, this study has certainly increased

our understanding of the extent to which a square's layout affects thermal comfort. Future research should investigate how to reduce PET by reorganizing the general arrangement while maintaining the same landscape element coverage. Interaction factors should also be added to further explore how multi-factor layouts can contribute to the thermal comfort of squares.

Nomenclature

UHI	Urban heat island
IPCC	Intergovernmental Panel on Climate Change
°C	Degrees Celsius
M	Meter
m^2	Square meter
AT	Air temperature (°C)
RH	Relative humidity (%)
WS	Wind speed (m/s)
A.D.	Anno Domini
RMSE	Root-mean-square deviation
R^2	Coefficient of determination
W	Water body
T	Vegetation
B	Buildings
SET*	Standard Effective Temperature
PMV	Predicted Mean Vote
UTCI	Universal Thermal Climate Index
PET	Physiological equivalent temperature
Spearman's ρ	Spearman's correlation coefficient

References

1. Goodess, C.; Berk, S.; Ratna, S.B.; Brousse, O.; Davies, M.; Heaviside, C.; Moore, G.; Pineo, H. Climate change projections for sustainable and healthy cities. *Build. Cities* **2021**, *2*, 812. [CrossRef]
2. Chaturvedi, S.; Cheong, T.S.; Luo, Y.; Singh, C.; Shaw, R. *IPCC Sixth Assessment Report (AR6): Climate Change 2022-Impacts, Adaptation and Vulnerability: Regional Factsheet Asia*; IPCC: Geneva, Switzerland, 2022.
3. Zheng, T.; Qu, K.; Darkwa, J.; Calautit, J.K. Evaluating urban heat island mitigation strategies for a subtropical city centre (a case study in Osaka, Japan). *Energy* **2022**, *250*, 123721. [CrossRef]
4. Molina-Gómez, N.I.; Varon-Bravo, L.M.; Sierra-Parada, R.; López-Jiménez, P.A. Urban growth and heat islands: A case study in micro-territories for urban sustainability. *Urban Ecosyst.* **2022**. [CrossRef]
5. Yang, X.; Gao, W.; Zhang, Q.; Li, S.; Fu, F.; Li, N. Analyzing the Environment Characteristics of Heat Exposure Spaces from the Humanistic Perspective and Spatial Improvement Approaches in Central Beijing, China. *Buildings* **2022**, *12*, 138. [CrossRef]
6. Hou, H.; Su, H.; Liu, K.; Li, X.; Chen, S.; Wang, W.; Lin, J. Driving forces of UHI changes in China's major cities from the perspective of land surface energy balance. *Sci. Total Environ.* **2022**, *829*, 154710. [CrossRef]

7.　Ozarisoy, B. Energy effectiveness of passive cooling design strategies to reduce the impact of long-term heatwaves on occupants' thermal comfort in Europe: Climate change and mitigation. *J. Clean. Prod.* **2022**, *330*, 129675. [CrossRef]

8.　Nasrollahi, N.; Ghosouri, A.; Khodakarami, J.; Taleghani, M. Heat-Mitigation Strategies to Improve Pedestrian Thermal Comfort in Urban Environments: A Review. *Sustainability* **2020**, *12*, 10000. [CrossRef]

9.　Lin, T.-P. Thermal perception, adaptation and attendance in a public square in hot and humid regions. *Build. Environ.* **2009**, *44*, 2017–2026. [CrossRef]

10.　Kariminia, S.; Ahmad, S.S. Dependence of Visitors' Thermal Sensations on Built Environments at an Urban Square. *Procedia-Soc. Behav. Sci.* **2013**, *85*, 523–534. [CrossRef]

11.　Kim, H.; Kim, S.W.; Jo, Y.; Kim, E.J. Findings from a field study of urban microclimate in Korea using mobile meteorological measurements. *Open House Int.* **2022**. *ahead-of-print*. [CrossRef]

12.　Battista, G.; de Lieto Vollaro, R.; Zinzi, M. Assessment of urban overheating mitigation strategies in a square in Rome, Italy. *Sol. Energy* **2019**, *180*, 608–621. [CrossRef]

13.　Elnabawi, M.H.; Hamza, N. Outdoor Thermal Comfort: Coupling Microclimatic Parameters with Subjective Thermal Assessment to Design Urban Performative Spaces. *Buildings* **2020**, *10*, 238. [CrossRef]

14.　Gagge, A.P.; Fobelets, A.P.; Berglund, L. A standard predictive index of human response to the thermal environment. *ASHRAE trans.* **1986**, *92*, 709–731.

15.　Höppe, P. The physiological equivalent temperature–A universal index for the biometeorological assessment of the thermal environment. *Int. J. Biometeorol.* **1999**, *43*, 71–75. [CrossRef]

16.　Sun, S.; Yu, Y. Dimension and formation of placeness of commercial public space in city center: A case study of Deji Plaza in Nanjing. *Front. Arch. Res.* **2021**, *10*, 229–239. [CrossRef]

17.　Liu, S.; Zhao, J.; Xu, M.; Ahmadian, E. Effects of landscape patterns on the summer microclimate and human comfort in urban squares in China. *Sustain. Cities Soc.* **2021**, *73*, 103099. [CrossRef]

18.　Zölch, T.; Rahman, M.A.; Pfleiderer, E.; Wagner, G.; Pauleit, S. Designing public squares with green infrastructure to optimize human thermal comfort. *Build. Environ.* **2019**, *149*, 640–654. [CrossRef]

19.　McRae, I.; Freedman, F.R.; Rivera, A.; Li, X.; Dou, J.; Cruz, I.; Ren, C.; Dronova, I.; Fraker, H.; Bornstein, R. Integration of the WUDAPT, WRF, and ENVI-met models to simulate extreme daytime temperature mitigation strategies in San Jose, California. *Build. Environ.* **2020**, *184*, 107180. [CrossRef]

20.　Stocco, S.; Cantón, M.A.; Correa, E. Evaluation of design schemes for urban squares in arid climate cities, Mendoza, Argentina. *Build. Simul.* **2021**, *14*, 763–777. [CrossRef]

21.　Ma, X.; Leung, T.; Chau, C.; Yung, E.H. Analyzing the influence of urban morphological features on pedestrian thermal comfort. *Urban Clim.* **2022**, *44*, 101192. [CrossRef]

22.　Yang, Y.; Zhang, X.; Lu, X.; Hu, J.; Pan, X.; Zhu, Q.; Su, W. Effects of Building Design Elements on Residential Thermal Environment. *Sustainability* **2017**, *10*, 57. [CrossRef]

23.　Shareef, S.; Abu-Hijleh, B. The effect of building height diversity on outdoor microclimate conditions in hot climate. A case study of Dubai-UAE. *Urban Clim.* **2020**, *32*, 100611. [CrossRef]

24.　Perini, K.; Magliocco, A. Effects of vegetation, urban density, building height, and atmospheric conditions on local temperatures and thermal comfort. *Urban For. Urban Green.* **2014**, *13*, 495–506. [CrossRef]

25.　Gaitani, N.; Spanou, A.; Saliari, M.; Synnefa, A.; Vassilakopoulou, K.; Papadopoulou, K.; Pavlou, K.; Santamouris, M.; Papaioannou, M.; Lagoudaki, A. Improving the microclimate in urban areas: A case study in the centre of Athens. *Build. Serv. Eng. Res. Technol.* **2011**, *32*, 53–71. [CrossRef]

26.　Zhang, T.; Hong, B.; Su, X.; Li, Y.; Song, L. Effects of tree seasonal characteristics on thermal-visual perception and thermal comfort. *Build. Environ.* **2022**, *212*, 108793. [CrossRef]

27.　Hong, B.; Lin, B. Numerical study of the influences of different patterns of the building and green space on micro-scale outdoor thermal comfort and indoor natural ventilation. *Build. Simul.* **2014**, *7*, 525–536. [CrossRef]

28.　Cong, Y.; Zhu, R.; Yang, L.; Zhang, X.; Liu, Y.; Meng, X.; Gao, W. Correlation Analysis of Thermal Comfort and Landscape Characteristics: A Case Study of the Coastal Greenway in Qingdao, China. *Buildings* **2022**, *12*, 541. [CrossRef]

29.　Jacobs, C.; Klok, L.; Bruse, M.; Cortesão, J.; Lenzholzer, S.; Kluck, J. Are urban water bodies really cooling? *Urban Clim.* **2020**, *32*, 100607. [CrossRef]

30.　Ma, X.; Fukuda, H.; Zhou, D.; Wang, M. Study on outdoor thermal comfort of the commercial pedestrian block in hot-summer and cold-winter region of southern China-a case study of The Taizhou Old Block. *Tour. Manag.* **2019**, *75*, 186–205. [CrossRef]

31.　Lai, D.; Lian, Z.; Liu, W.; Guo, C.; Liu, W.; Liu, K.; Chen, Q. A comprehensive review of thermal comfort studies in urban open spaces. *Sci. Total Environ.* **2020**, *742*, 140092. [CrossRef]

32.　Lai, D.; Liu, W.; Gan, T.; Liu, K.; Chen, Q. A review of mitigating strategies to improve the thermal environment and thermal comfort in urban outdoor spaces. *Sci. Total Environ.* **2019**, *661*, 337–353. [CrossRef]

33.　Xi, T.; Wang, Q.; Qin, H.; Jin, H. Influence of outdoor thermal environment on clothing and activity of tourists and local people in a severely cold climate city. *Build. Environ.* **2020**, *173*, 106757. [CrossRef]

34.　Jia, S.; Wang, Y. Effect of heat mitigation strategies on thermal environment, thermal comfort, and walkability: A case study in Hong Kong. *Build. Environ.* **2021**, *201*, 107988. [CrossRef]

35. Li, J.; Liu, N. The perception, optimization strategies and prospects of outdoor thermal comfort in China: A review. *Build. Environ.* **2020**, *170*, 106614. [CrossRef]
36. Gao, Y.; Gao, W.; Meng, X.; Long, E. *Code for Thermal Design of Civil Buildings*; China Planning Press: Beijing, China, 1993.
37. Hui, Z.; Zeng, B. Research on Approaches and Significance of Great Wild Goose Pagoda Tourism under the Guidance of "the Belt and Road" Strategy. In Proceedings of the 2nd International Conference on Contemporary Education, Social Sciences and Humanities (ICCESSH 2017), Moscow, Russia, 14–15 June 2017; Atlantis Press: Amsterdam, The Netherlands, 2017.
38. Bruse, M.; Fleer, H. Simulating surface–plant–air interactions inside urban environments with a three dimensional numerical model. *Environ. Model. Softw.* **1998**, *13*, 373–384. [CrossRef]
39. Karimi, A.; Sanaieian, H.; Farhadi, H.; Norouzian-Maleki, S. Evaluation of the thermal indices and thermal comfort improvement by different vegetation species and materials in a medium-sized urban park. *Energy Rep.* **2020**, *6*, 1670–1684. [CrossRef]
40. Chen, Z.J. *Research of Vegetation System's Effects on Outdoor Thermal Environment of Residential Communities in Hot-Humid Climate*; South China University of Technology: Guangzhou, China, 2010.
41. Salata, F.; Golasi, I.; de Lieto Vollaro, R.; de Lieto Vollaro, A. Urban microclimate and outdoor thermal comfort. A proper procedure to fit ENVI-met simulation outputs to experimental data. *Sustain. Cities Soc.* **2016**, *26*, 318–343. [CrossRef]
42. Yang, S.; Zhou, D.; Wang, Y.; Li, P. Comparing impact of multi-factor planning layouts in residential areas on summer thermal comfort based on orthogonal design of experiments (ODOE). *Build. Environ.* **2020**, *182*, 107145. [CrossRef]
43. Zhang, H.; Chen, B.; Sun, Z.; Bao, Z. Landscape perception and recreation needs in urban green space in Fuyang, Hangzhou, China. *Urban For. Urban Green.* **2013**, *12*, 44–52. [CrossRef]
44. Theeuwes, N.E.; Solcerová, A.; Steeneveld, G.J. Modeling the influence of open water surfaces on the summertime temperature and thermal comfort in the city. *J. Geophys. Res. Atmos.* **2013**, *118*, 8881–8896. [CrossRef]
45. Liu, B.; Lian, Z.; Brown, R.D. Effect of Landscape Microclimates on Thermal Comfort and Physiological Wellbeing. *Sustainability* **2019**, *11*, 5387. [CrossRef]
46. *CJJT 85-2017*; Classification Standard of Urban Green Space (CJJT 85-2017). Code of China: Beijing, China, 2019.
47. Chen, G.; Rong, L.; Zhang, G. Unsteady-state CFD simulations on the impacts of urban geometry on outdoor thermal comfort within idealized building arrays. *Sustain. Cities Soc.* **2021**, *74*, 103187. [CrossRef]
48. Hong, B.; Lin, B. Numerical studies of the outdoor wind environment and thermal comfort at pedestrian level in housing blocks with different building layout patterns and trees arrangement. *Renew. Energy* **2015**, *73*, 18–27. [CrossRef]
49. Olesen, B.W.; Brager, G.S. *A Better Way to Predict Comfort: The New ASHRAE Standard 55-2004*; UC Berkeley: Berkeley, CA, USA, 2004.
50. Auliciems, A.; Szokolay, S.V. Thermal Comfort. PLEA sl. 1997. Available online: https://labeee.ufsc.br/sites/default/files/disciplinas/Szokolay%20e%20Auliciems,%201997.pdf (accessed on 4 June 2022).
51. Migliari, M.; Babut, R.; De Gaulmyn, C.; Chesne, L.; Baverel, O. The Metamatrix of Thermal Comfort: A compendious graphical methodology for appropriate selection of outdoor thermal comfort indices and thermo-physiological models for human-biometeorology research and urban planning. *Sustain. Cities Soc.* **2022**, *81*, 103852. [CrossRef]
52. Yao, R.; Zhang, S.; Du, C.; Schweiker, M.; Hodder, S.; Olesen, B.W.; Toftum, J.; D'Ambrosio, F.R.; Gebhardt, H.; Zhou, S.; et al. Evolution and performance analysis of adaptive thermal comfort models—A comprehensive literature review. *Build. Environ.* **2022**, *217*, 109020. [CrossRef]
53. Coccolo, S.; Kämpf, J.; Scartezzini, J.-L.; Pearlmutter, D. Outdoor human comfort and thermal stress: A comprehensive review on models and standards. *Urban Clim.* **2016**, *18*, 33–57. [CrossRef]
54. Zhang, Y.; Liu, C. Digital Simulation for Buildings' Outdoor Thermal Comfort in Urban Neighborhoods. *Buildings* **2021**, *11*, 541. [CrossRef]
55. Jendritzky, G.; Maarouf, A.; Fiala, D.; Staiger, H. An update on the development of a Universal Thermal Climate Index. In Proceedings of the 15th Conference on Biometeorology/Aerobiology and 16th International Congress of Biometeorology, Kansas City, MO, USA, 29 October 2002.
56. Kumar, P.; Sharma, A. Study on importance, procedure, and scope of outdoor thermal comfort—A review. *Sustain. Cities Soc.* **2020**, *61*, 102297. [CrossRef]
57. Fischereit, J.; Schlünzen, K.H. Evaluation of thermal indices for their applicability in obstacle-resolving meteorology models. *Int. J. Biometeorol.* **2018**, *62*, 1887–1900. [CrossRef]
58. Yu, H.; Fukuda, H. A Review of Outdoor Thermal Comfort Indices in Northern China (Urban Built Environment beyond the Global Pandemic). In Proceedings of the 17th International Conference of Asia Institute of Urban Environment, Virtual, 19–20 December 2020; pp. 177–180.
59. Xu, M.; Hong, B.; Mi, J.; Yan, S. Outdoor thermal comfort in an urban park during winter in cold regions of China. *Sustain. Cities Soc.* **2018**, *43*, 208–220. [CrossRef]
60. Tian, Y.; Hong, B.; Zhang, Z.; Wu, S.; Yuan, T. Factors influencing resident and tourist outdoor thermal comfort: A comparative study in China's cold region. *Sci. Total Environ.* **2022**, *808*, 152079. [CrossRef] [PubMed]
61. Ozarisoy, B.; Altan, H. Regression forecasting of 'neutral' adaptive thermal comfort: A field study investigation in the southeastern Mediterranean climate of Cyprus. *Build. Environ.* **2021**, *202*, 108013. [CrossRef]
62. Chen, Q.; Lin, C.; Guo, D.; Hou, Y.; Lai, D. Studies of outdoor thermal comfort in northern China. *Build. Environ.* **2014**, *77*, 110–118.

63. Yang, J.; Hu, X.; Feng, H.; Marvin, S. Verifying an ENVI-met simulation of the thermal environment of Yanzhong Square Park in Shanghai. *Urban For. Urban Green.* **2021**, *66*, 127384. [CrossRef]
64. Al-Bdour, M.; Baranyai, B. An overview of microclimate tools for predicting the thermal comfort, meteorological parameters and design strategies in outdoor spaces. *Pollack Period.* **2019**, *14*, 109–118. [CrossRef]
65. Tsoka, S.; Tsikaloudaki, A.; Theodosiou, T. Analyzing the ENVI-met microclimate model's performance and assessing cool materials and urban vegetation applications–A review. *Sustain. Cities Soc.* **2018**, *43*, 55–76. [CrossRef]
66. Sodoudi, S.; Zhang, H.; Chi, X.; Müller, F.; Li, H. The influence of spatial configuration of green areas on microclimate and thermal comfort. *Urban For. Urban Green.* **2018**, *34*, 85–96. [CrossRef]
67. de Freitas, W.K.; Magalhães, L.M.S.; de Santana, C.A.A.; Junior, E.R.P.; de Souza, L.D.C.M.; Toledo, R.A.B.; Garção, B.R. Tree composition of urban public squares located in the Atlantic Forest of Brazil: A systematic review. *Urban For. Urban Green.* **2020**, *48*, 126555. [CrossRef]
68. Morakinyo, T.E.; Kong, L.; Lau, K.K.L.; Yuan, C.; Ng, E. A study on the impact of shadow-cast and tree species on in-canyon and neighborhood's thermal comfort. *Build. Environ.* **2017**, *115*, 1–17. [CrossRef]
69. Morakinyo, T.E.; Lam, Y.F. Simulation study on the impact of tree-configuration, planting pattern and wind condition on street-canyon's micro-climate and thermal comfort. *Build. Environ.* **2016**, *103*, 262–275. [CrossRef]
70. Hong, B.; Lin, B.; Qin, H. Numerical investigation on the coupled effects of building-tree arrangements on fine particulate matter (PM2.5) dispersion in housing blocks. *Sustain. Cities Soc.* **2017**, *34*, 358–370. [CrossRef]
71. Spearman's Rank Correlation Coefficient. 1988. Available online: https://en.wikipedia.org/wiki/Spearman%27s_rank_correlation_coefficient (accessed on 5 May 2022).
72. Gauthier, T.D. Detecting trends using Spearman's rank correlation coefficient. *Environ. Forensics* **2001**, *2*, 359–362. [CrossRef]